

# Microscopic calculation of neutrino mean free path inside hot neutron matter

Jérôme Margueron

GANIL CEA/DSM - CNRS/IN2P3 BP 5027 F-14076 Caen CEDEX 5, France

Isaac Vidaña and Ignazio Bombaci

Dipartimento di Fisica “Enrico Fermi”, Università di Pisa and  
INFN Sezione di Pisa, Via Buonarroti 2, I-56127 Pisa, Italy

(Dated: October 30, 2018)

We calculate the neutrino mean free path and the Equation of State of pure neutron matter at finite temperature within a selfconsistent scheme based on the Brueckner–Hartree–Fock approximation. We employ the nucleon-nucleon part of the recent realistic baryon-baryon interaction (model NSC97e) constructed by the Nijmegen group. The temperatures considered range from 10 to 80 MeV. We report on the calculation of the mean field, the residual interaction and the neutrino mean free path including short and long range correlations given by the Brueckner–Hartree–Fock plus Random Phase Approximation (BHF+RPA) framework. This is the first fully consistent calculation in hot neutron matter dedicated to neutrino mean free path. We compare systematically our results to those obtained with the D1P Gogny effective interaction, which is independent of the temperature. The main differences between the present calculation and those with nuclear effective interactions come from the RPA corrections to BHF (a factor of about 8) while the temperature lack of consistency accounts for a factor of about 2.

PACS numbers: 26.60.+c, 26.50.+x

Keywords: neutrino mean free path, neutron star, supernovae, Brueckner–Hartree–Fock, RPA

## I. INTRODUCTION

Neutrinos play a crucial role in the physics of supernova explosions [1] and in the early evolution of their compact stellar remnants [2, 3]. During the collapse of the pre-supernova core, a large number of neutrinos is produced by electron capture process. The mean free path  $\lambda$  of these neutrinos decreases as the radius of the newly formed neutron star shrinks from about 100 km to about 10 km, becoming smaller than the stellar radius when density reaches a critical value (*neutrino trapping density*). Under these conditions neutrinos are *trapped* in the star. Neutrino trapping has a strong influence on the overall *stiffness* of the dense matter Equation of State (EoS) [4, 5], being the physical conditions of the hot and lepton-rich newborn neutron star substantially different from those of the cold and deleptonized neutron star.

The scattering of neutrinos on neutrons is mediated by the neutral current of the electroweak interaction. In the non-relativistic limit for neutrons, the mean free path of a neutrino with initial energy  $E_\nu$  is given by [6]

$$\lambda^{-1}(E_\nu, T) = \frac{G_F^2}{16\pi^2} \int d\mathbf{k}_3 \left( c_V^2 (1 + \cos \theta) \mathcal{S}^{(0)}(q, T) + c_A^2 (3 - \cos \theta) \mathcal{S}^{(1)}(q, T) \right), \quad (1)$$

where  $T$  is the temperature,  $G_F$  is the Fermi constant,  $c_V$  ( $c_A$ ) the vector (axial) coupling constant,  $k_1 = (E_\nu, \mathbf{k}_1)$  and  $k_3$  are the initial and final neutrino four-momenta,  $q = k_1 - k_3$  the transferred four-momentum, and  $\cos \theta = \hat{\mathbf{k}}_1 \cdot \hat{\mathbf{k}}_3$ . In the following, we impose the average energy  $E_\nu = 3T$  [7]. The dynamical structure factors  $\mathcal{S}^{(S)}(q, T)$

describe the response of neutron matter to excitations induced by neutrinos, and they contain the relevant information on the medium (cf Eq. 16). The vector (axial) part of the neutral current gives rise to density (spin-density) fluctuations, corresponding to the  $S = 0$  ( $S = 1$ ) spin channel.

In this paper, we report on calculations of the mean free path of neutrinos in pure neutron matter under various conditions of density and temperature. A microscopic framework based on the Brueckner–Hartree–Fock (BHF) approximation of the Brueckner–Bethe–Goldstone (BBG) theory is employed to describe consistently both the EoS and the dynamical structure factors of neutron matter including finite temperature effects.

The paper is organized in the following way. A brief review of the BHF approximation at zero temperature and its extension to the finite temperature case is presented in Sec. II. The Landau parameters  $F_0, F_1, G_0$  and  $G_1$  are calculated in Sec. III. Section IV is devoted to the calculation of the dynamical structure factors and the neutrino mean free path. Finally, the main conclusions of this work are drawn in Sec. V.

## II. EOS AT FINITE TEMPERATURE

Our many-body scheme is based on the BHF approximation of the BBG theory. It starts with the construction of the neutron-neutron  $G$ -matrix, which describes in an effective way the interaction between two neutrons in the presence of a surrounding medium. It is formally obtained by solving the well known Bethe–Goldstone equa-

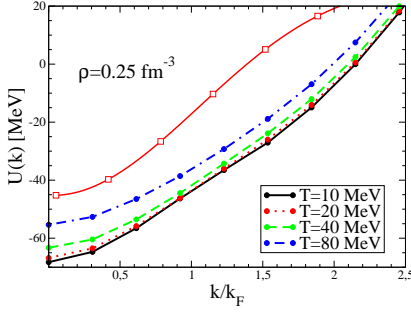


FIG. 1: Mean field for several temperatures as a function of the momentum  $k$  in units of  $k_F$ . The result of Brueckner-Hartree-Fock calculation is represented with filled circles while the mean field given by the D1P Gogny effective interaction is represented with empty squares.

tion, written schematically as

$$G(\omega) = V + V \frac{Q}{\omega - E_1 - E_2 + i\eta} G(\omega) . \quad (2)$$

In the above expression  $V$  denotes the bare interaction,  $Q$  is the Pauli operator which allows only intermediate states compatible with the Pauli principle, and  $\omega$ , the so-called starting energy, corresponds to the sum of non-relativistic single-particle energies of the interacting neutrons. The single-particle energy  $E$  is given by

$$E(k) = \frac{\hbar^2 k^2}{2m} + U(k) , \quad (3)$$

where the single-particle potential  $U(k)$  represents the mean field “felt” by the neutron due to its interaction with the other neutrons of the medium. In the BHF approximation  $U(k)$  is given by

$$U(k) = \text{Re} \sum_{k'} n(k') \left\langle \vec{k} \vec{k}' \right| G(\omega = E(k) + E(k')) \left| \vec{k} \vec{k}' \right\rangle_{\mathcal{A}} \quad (4)$$

where

$$n(k) = \begin{cases} 1, & \text{if } k \leq k_F \\ 0, & \text{otherwise} \end{cases} \quad (5)$$

is the corresponding occupation number and the matrix elements are properly antisymmetrized. The resulting single-particle potential is shown together with the corresponding one for the D1P Gogny [8] effective interaction in Fig. 1 for  $\rho = 0.25 \text{ fm}^{-3}$  ( $k_F = 1.95 \text{ fm}^{-3}$ ). We note here that the so-called continuous prescription has been adopted for the single-particle potential when solving the Bethe–Goldstone equation. As shown by the authors of Refs. [9, 10], the contribution to the energy per particle from three-body clusters is diminished in this prescription. We note also that the present calculations have been carried out by using the nucleon-nucleon part of the recent realistic baryon-baryon interaction (model NSC97e) constructed by the Nijmegen group [11]. The

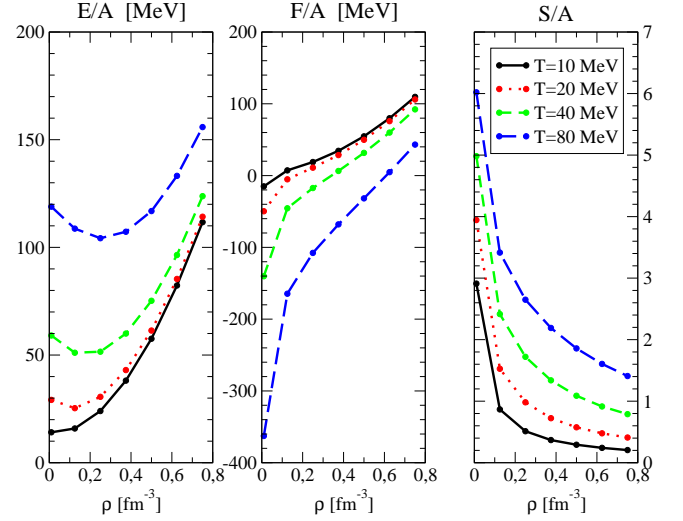


FIG. 2: Energy per particle, free energy per particle and entropy per particle as a function of the number density for several temperatures.

total energy per particle,  $E/A$ , is easily calculated once a self-consistent solution of Eqs. (2)–(4) is achieved

$$\frac{E}{A} = \frac{1}{A} \sum_k n(k) \left( \frac{\hbar^2 k^2}{2m} + \frac{1}{2} U(k) \right) . \quad (6)$$

The many-body problem at finite temperature has been considered by several authors within different approaches, such as the finite temperature Green’s function method [12], the thermo-field method [13], or the Bloch–De Dominicis (BD) diagrammatic expansion [14]. The latter, developed soon after the Brueckner theory, represents the “natural” extension to finite temperature of the BBG expansion, to which it leads in the zero temperature limit. Baldo and Ferreira [15] showed that the dominant terms in the BD expansion were those that correspond to the zero temperature BBG diagrams, where the temperature is introduced only through the Fermi-Dirac distribution

$$f(k, T) = \frac{1}{1 + \exp([E(k, T) - \mu_n(T)]/T)} . \quad (7)$$

Therefore, at the BHF level, finite temperature effects can be introduced in a very good approximation just replacing in the Bethe–Goldstone equation: (i) the zero temperature Pauli operator  $Q = (1 - n_1)(1 - n_2)$  by the corresponding finite temperature one  $Q(T) = (1 - f_1)(1 - f_2)$ , and (ii) the single-particle energies  $E(k)$  by the temperature dependent ones  $E(k, T)$  obtained from Eqs. (3-4) when  $n(k)$  is replaced by  $f(k, T)$ .

In this case, however, the self-consistent process implies that together with the Bethe–Goldstone equation and the single-particle potential, the chemical potential of the neutron,  $\mu_n(T)$ , must be extracted at each step of

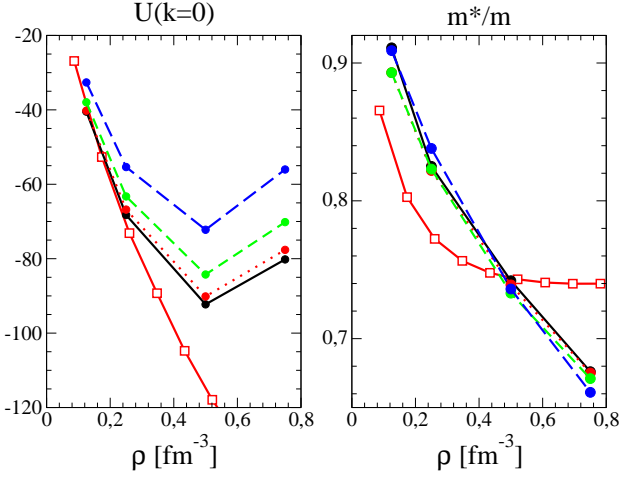


FIG. 3: Quadratic approximation of the single-particle energy:  $U(k=0)$  is the constant mean field and  $m^*$  is the effective mass. See Fig. 1 for the legend.

the iterative process from the normalization condition

$$\rho = \sum_k f(k, T) . \quad (8)$$

This is an implicit equation which can be solved numerically by e.g., the Newton–Raphson method. Note that, now, also the Bethe–Goldstone equation and single-particle potential depend implicitly on the chemical potential.

Once a self-consistent solution is obtained the total free energy per particle is determined by

$$\frac{F}{A} = \frac{E}{A} - T \frac{S}{A} , \quad (9)$$

where  $E/A$  is evaluated from Eq. (6) replacing  $n(k)$  by  $f(k, T)$  and the total entropy per particle,  $S/A$ , is calculated through the expression

$$\begin{aligned} \frac{S}{A} = & -\frac{1}{A} \sum_k [f(k, T) \ln(f(k, T)) \\ & + (1 - f(k, T)) \ln(1 - f(k, T))] . \end{aligned} \quad (10)$$

Results for the quantities  $E/A$ ,  $F/A$  and  $S/A$  are shown in Fig. 2 for several densities and temperatures.

The  $k$ -momentum dependence of the single-particle energy is usually approximated by a quadratic function which consist in a constant term, the mean field, and a squared momentum dependent term, related to the neutron effective mass  $m^*$ , reading

$$E^{\text{eff}}(k) \equiv \frac{\hbar^2 k^2}{2m^*} + U(k=0) \quad (11)$$

where

$$\frac{\hbar}{m^*} = \frac{\hbar}{m} + \frac{1}{k} \frac{\partial U(k)}{\partial k} \Big|_{k=k_F} \quad (12)$$

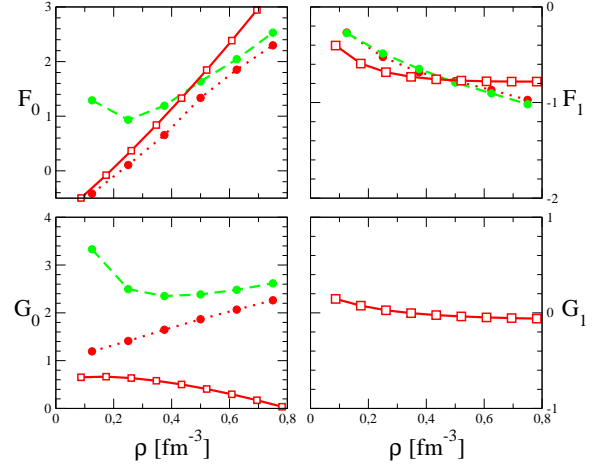


FIG. 4: Landau parameters deduced for  $T=10$  MeV (dotted line) and  $80$  MeV (dashed line) using the Nijmegen potential. It is compared with the one deduced from the D1P Gogny interaction (empty squares).

We finish this section by showing in Fig. 3 the mean field and the effective mass as a function of the density, for several temperatures. As the temperature increases, the value of the mean field also increases. One can remark that the effective mass is nearly independent of the temperature up to  $T=80$  MeV.

### III. LANDAU PARAMETERS $F_0$ , $F_1$ , $G_0$ AND $G_1$

The Landau parameters  $F_0$ ,  $G_0$  are related to the incompressibility modulus  $K$  and the magnetic susceptibility  $\chi$  respectively through

$$K = 9\rho \frac{\partial^2 F/V}{\partial \rho^2} = 9\rho \frac{1 + F_0}{N_0} , \quad (13)$$

$$\chi^{-1} = \frac{1}{(\mu\rho)^2} \frac{\partial^2 F/V}{\partial \rho_s^2} = \frac{1 + G_0}{\chi_F} , \quad (14)$$

where  $F/V = (F/A)\rho$  is the free energy density,  $N_0 = m^* k_F / \pi^2 \hbar^2$  is the density of states,  $\chi_F$  is the magnetic susceptibility of a free Fermi gas and  $\rho_s = \rho_\uparrow - \rho_\downarrow$  is the spin asymmetry density (i.e., the difference in the densities of neutrons with spin up and spin down). The parameter  $F_1$  is deduced from the effective mass according to the relation

$$\frac{m^*}{m} = 1 + \frac{F_1}{3} . \quad (15)$$

There is no simple relation for the Landau parameter  $G_1$  that can be deduced from thermodynamical properties or general relations like the forward scattering sum rule. Gogny effective interaction predicts that  $G_1$  is close to zero at all densities (cf Fig. 4), hence, we will assume in the following that  $G_1=0$ .

Finally, the Landau parameters we obtain in pure neutron matter are shown on Fig. 4. The absolute values of  $F_0$  and  $G_0$  increase with the temperature while  $F_1$  is nearly constant. The main differences between the Landau parameters calculated with the BHF approximation and those calculated with the Gogny effective interaction, are present in the spin fluctuation channel. In the latter case, for high densities, the Landau parameter  $G_0$  falls to  $-1$  because of a ferromagnetic instability [16] while  $G_0$  increase with density for the BHF calculation, since no such an instability is found in this case [17].

#### IV. DYNAMICAL STRUCTURE FACTORS AND NEUTRINO MEAN FREE PATH

We obtain the dynamical structure factors  $\mathcal{S}^{(S)}$  from the imaginary part of the response function  $\chi^{(S)}(q, T)$  in pure neutron matter as [18]

$$\mathcal{S}^{(S)}(q, q_0, T) = -\frac{1}{\pi} \frac{1}{1 - \exp(-q_0/T)} \Im \chi^{(S)}(q, q_0, T). \quad (16)$$

In the Brueckner–Hartree–Fock (BHF) approximation the response function is given by

$$\Im \chi_{\text{BHF}}^{(S)}(q, q_0, T) = -\frac{m^* T}{4\pi q} \ln \left( \frac{1 + e^{(A+q_0/2)/T}}{1 + e^{(A-q_0/2)/T}} \right), \quad (17)$$

where  $A = \mu_n - m^*/2(q_0/q)^2 - q^2/8m^*$ . This expression is valid for both positive and negative transferred energies  $q_0$ . The real and imaginary part of the response function have been obtained within the quadratic approximation for the single-particle energy (see Eq. (11)). The influence of the in-medium interaction appears through the effective mass  $m^*$  and the chemical potential  $\mu_n$ , which introduce, besides a density dependence, an additional temperature dependence in the response function.

We have also included the long range correlations within the BHF+RPA scheme. The particle-hole interaction is approached by a Landau form, containing only  $l = 0$  multipole (RPA  $l = 0$ ), or  $l = 0, 1$  multipoles (RPA  $l = 0, 1$ ) [19]. We stress that in all cases the particle-hole interaction has been consistently obtained from the particle-particle interaction used to describe the EoS.

The dynamical structure factors, within the BHF and BHF+RPA scheme, are displayed in Fig. 5 and Fig. 6 as a function of the transferred energy  $q_0$  and for  $\rho = 0.25 \text{ fm}^{-3}$ ,  $T = 10 \text{ MeV}$  and  $q = 10 \text{ MeV}$ . In Fig. 6 we show the dynamical structure factors for the density ( $S = 0$ ) and spin-density ( $S = 1$ ) channels. We compare the response function obtained with the Brueckner input (filled circle) to the result with the D1P Gogny effective interaction (empty square). The two columns correspond to two truncations in the BHF+RPA calculation which consist to include only the  $l = 0$  Landau parameters or the  $l = 0, 1$  Landau parameters. As expected from the values of the Landau parameters (cf Fig. 4), the main differences between the approaches are present in the spin channel

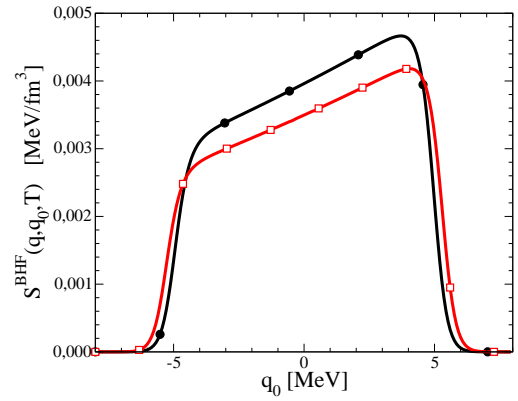


FIG. 5: Dynamical structure factors at the BHF approximation as a function of the transferred energy  $q_0$ , and for  $\rho = 0.25 \text{ fm}^{-3}$ ,  $T = 10 \text{ MeV}$  and  $q = 10 \text{ MeV}$ .

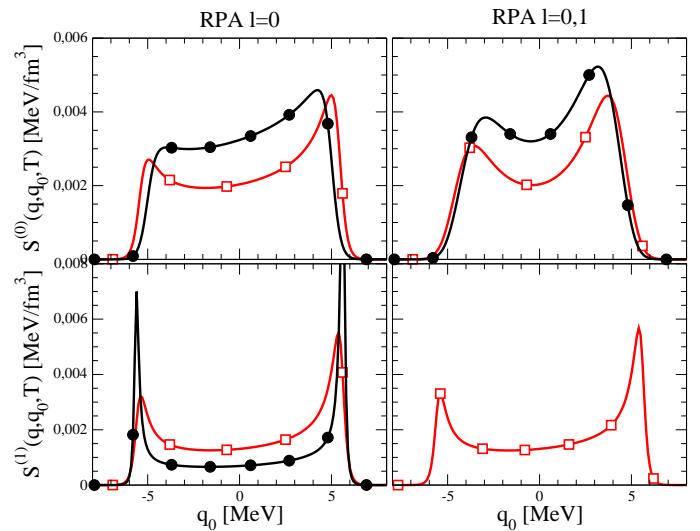


FIG. 6: Dynamical structure factors, for the channel  $S = 0$  and  $S = 1$ , as a function of the transferred energy  $q_0$ , and for  $\rho = 0.25 \text{ fm}^{-3}$ ,  $T = 10 \text{ MeV}$  and  $q = 10 \text{ MeV}$ .

( $S = 1$ ). The spin sound is weakly present for the D1P Gogny effective interaction while it seems very important for the Brueckner calculation. The pronounced zero sound in the spin-density channel at zero temperature is damped when the temperature increases, and these differences disappear at high temperature.

The density and temperature dependence of the neutrino mean free path is shown in Fig. 7. We have also performed a comparison with Gogny prediction. The behaviour of the mean free path follows approximatively the expected law in  $T^{-2}$  [7]. At low temperature, the discrepancies between the two interactions are essentially due to the density dependence of the effective mass (cf Eq. 17). Moreover, as the effective mass is independent of the temperature, a calculation of the in-medium interaction at finite temperature is not necessary. Hence, within BHF scheme, the mean free path is sensible to the tem-

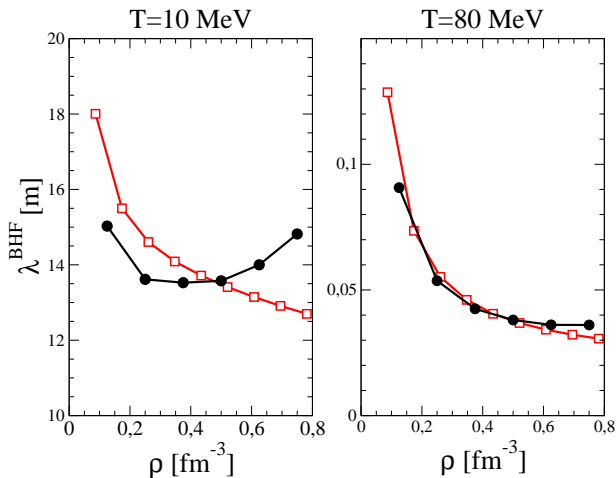


FIG. 7: The neutrino mean free path deduced from BHF response function as a function of the density for  $T=10$  MeV (left) and  $T=80$  MeV (right). The energy of the incoming neutrino is  $E_\nu = 3T$ .

perature essentially through the explicit  $T$ -dependance of the response function and the effect due to the finite temperature EoS is negligible. At high temperature, the 2 interactions gives very similar results because the effects of the medium are reduced ( $E_\nu = 3T$ ).

The effects of the residual interaction, i.e., of RPA correlations, can be seen in Fig. 8, where we have represented the ratio  $R = \lambda^{\text{BHF+RPA } l=0,1} / \lambda^{\text{BHF}}$  of the neutrino mean free path within BHF+RPA  $l = 0, 1$  to BHF as a function of the density. The solid line stands for  $T=10$  MeV and the dotted line for  $T=80$  MeV. The ratio  $R$  with Nijmegen potential is about 8 at high density while it is only 1 with Gogny interaction. This effect have also been shown for zero temperature EoS with three-body forces [20]. This is due to the presence of spin instabilities at high density in the case of Gogny interaction [19, 21]. These instabilities lead to the divergence of the dynamical form factor [16], hence the neutrino mean free path goes to zero. This illustrate the sensibility of the neutrino mean free path with the onset of instabilities. Here, it reduces the mean free path by a factor 8 at high density.

In order to understand the interplay between the explicit  $T$ -dependance of the response function (cf Eq. 17) and the Landau parameters calculated at finite temperature, we have broken the consistency of the approach. In Fig. 8, the solid line stands for a consistent calculation at  $T=10$  MeV while the dashed line stands for the calculation of the neutrino mean free path using low temperature Landau parameters ( $T=10$  MeV) but calculating the dynamical response function at  $T=80$  MeV. Hence, by comparing the solid and the dashed line calculated with the same particle-hole residual interaction, we see that the increase of temperature reduces the effect of the correlations. As an illustration, the increase of the temperature suppress the collective modes. The

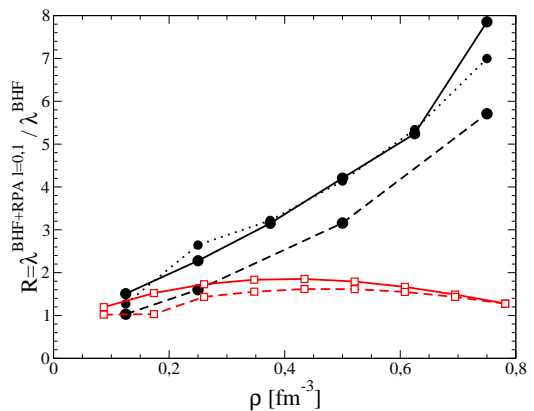


FIG. 8: Effects of BHF+RPA  $l = 0, 1$  for Brueckner (filled circle) and Gogny interactions (empty square). The solid line stands for a consistent calculation at  $T=10$  MeV, the dashed line is for  $T=80$  MeV but with the EoS at  $T=10$  MeV (consistency broken) and the dotted line is for  $T=80$  MeV (consistent). The energy of the incoming neutrino is  $E_\nu = 3T$ .

increase of temperature induce also the increase of the incoming neutrino energy ( $E_\nu = 3T$ ). The lack of consistency between finite temperature EoS and the dynamical response function leads to an underestimation of the neutrino mean free path of about 30-50%. The effect of restauring the temperature consistency for  $T=80$  MeV is illustrated by comparing the dashed line and the dotted line (consistent calculation for  $T=80$  MeV). As it has been shown on Fig. 4, the Landau parameters  $F_0$  and  $G_0$  increase with the temperature. The correlations become more important and the ratio  $R$  increase. Finally, the temperature induce two opposite effects: it increases the particle-hole interaction, but it decreases the effects of these correlations in the calculation of the dynamical structure factors. These two effects tend to compensate each other and the ratio  $R$ , at low temperature, is close to the ratio at high temperature.

## V. CONCLUSIONS

The purpose of this article is to study consistently the effects of the temperature to compute the neutrino mean free path in dense neutron matter. Both the EoS and the response function have been computed, including the BHF+RPA correlations. We have shown that the effective mass is nearly independent of the temperature.

We have shown the interplay between the effects of temperature for the calculation of the EoS (the mean field and residual interaction deduced from it) and the explicit temperature dependance of the dynamical structure factor. The first one increases the correlations with the temperature while the second one decreases it. Finally, these two opposite effects approximatively compensate each other and the ratio  $R$  is nearly constant for the range of temperature 10-80 MeV.

The temperature consistency does not change the general behaviour of the neutrino mean free path. The lack of consistency leads to an underestimation of the neutrino mean free path of about 30-50% for  $T=80$  MeV.

### Acknowledgements

The authors are very grateful to professor J. Navarro for useful discussions and comments. One of the authors

(J.M.) wishes to acknowledge the hospitality and support of the Istituto Nazionale di Fisica Nucleare, sezione di Pisa (Italy).

- 
- [1] H.-Th. Janka and E. Müller, *A&A* **306** (1996) 167.
  - [2] A. Burrows and J. M. Lattimer, *ApJ* **307** (1986) 178.
  - [3] H.-Th. Janka and E. Müller, *ApJ* **448** (1995) L109.
  - [4] I. Bombaci, *A&A* **305** (1996) 871.
  - [5] M. Prakash, I. Bombaci, M. Prakash, P.J. Ellis, J.M. Lattimer and R. Knorren, *Phys. Rep.* **280** (1997) 1.
  - [6] N. Iwamoto and C.J. Pethick, *Phys. Rev.* **D 25** (1982) 313.
  - [7] S. Reddy, M. Prakash and J.M.Lattimer, *Phys. Rev.* **D 58** (1998) 013009.
  - [8] M.Farine, D.Van-Eiff, P.Schuck, J.-F.Berger, J.Dechargé, and M.Girod, *J.Phys.G : Nucl.Part.Phys.* **25** (1999) 863.
  - [9] H. Q. Song, M. Baldo, G. Giansiracusa and U. Lombardo, *Phys. Rev. Lett.* **81**, 1584 (1998).
  - [10] M. Baldo, G. Giansiracusa, U. Lombardo and H. Q. Song, *Phys. Lett. B* **473**, 1 (2000).
  - [11] V. G. J. Stoks and Th. A. Rijken, *Phys. Rev. C* **59** (1999) 3009.
  - [12] A. L. Fetter and J. D. Walecka, *Quantum Theory of Many Particle Physics* (McGraw-Hill, New York, 1971).
  - [13] P. A. Hening, *Phys. Rep.* **253** (1995) 235.
  - [14] C. Bloch, *Nucl. Phys.* **7** (1958) 451; C. Bloch and C. De Domicis, *ibid* **7** (1958) 459; **10** (1959) 181; **10** (1959) 509.
  - [15] M. Baldo and L.S. Ferreira, *Phys. Rev. C* **59** (1999) 682.
  - [16] J. Margueron, J.Navarro and N. Van Giai, *Phys. Rev. C* **66** (2002) 014303.
  - [17] I. Vidaña, A. Polls and A. Ramos, *Phys. Rev. C* **65** (2002) 035804.
  - [18] J. Navarro, E.S. Hernández and D. Vautherin, *Phys. Rev. C* **60** (1999) 045801.
  - [19] J. Margueron, J.Navarro, W.Z. Jiang and N. Van Giai, "The nuclear Many-Body Problem 2001", NATO Sciences Series II (Kluwer Academic Publish); nucl-th/0110026.
  - [20] U. Lombardo, C. Shen N. Van Giai and W. Zuo, proceeding of International Symposium on Physics of Unstable Nuclei, Halong Bay (Vietnam) Nov. 2002.
  - [21] J. Margueron, J. Navarro and N.V. Giai, *Nucl. Phys. A* **719** (2003) 169c.